



Large Aperture Permanent Magnet Wiggler for the ILC Damping Rings

A. Babayan¹, M. Preger²

February 05, 2007

Abstract

In order to ensure large dynamic aperture to the ILC Damping Rings, the harmonic content of the wiggler field must be reduced with respect to the previous design. A new configuration with enlarged pole width and gap is here proposed.

¹ YerPhI, Yerevan, Armenia

² INFN-LNF, Frascati, Italy

1 Magnetic structure

The first proposal for a permanent magnet wiggler for the ILC Damping Rings [1] consisted of a hybrid structure with a period length of 400 mm, a pole width of 60 mm and a gap of 25 mm. To further improve the field quality, we propose here a new design, with the pole width increased to 80 mm and the gap height to 32 mm. In this way the good field region is enlarged from 20 to 28 mm. The new value for the wiggler gap comes from the optimization of the weight of the entire structure, which is obviously connected to its overall cost. Details of the magnetic design are illustrated in Figs.1,2. The cross section of the whole structure is 280x432 mm². The poles have a size of 100x80x110 mm³ (LxWxH) with a symmetric chamfer of 5 mm corresponding to the pole overhang in the gap region, and are made out of low carbon steel.

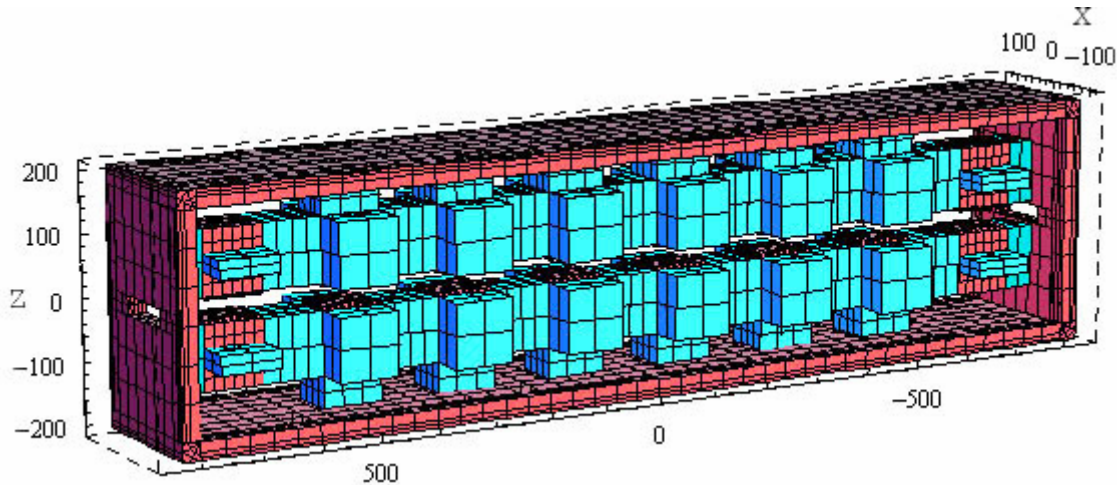


Fig.1: Wiggler magnet structure (three full periods + 2 half poles) shown without iron yoke sides

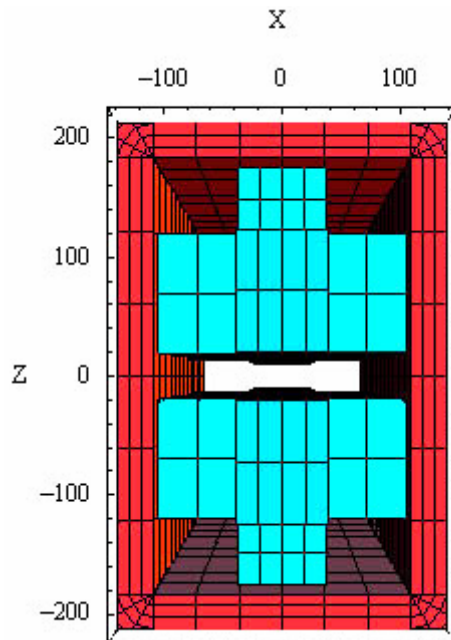


Fig.2: Front view of the wiggler without front iron yokes.
The transverse size of the device is 280x432 mm².

NdFeB with a remanent field of $Mr \sim 1.25$ T is used for the axial, side and top magnets of $100 \times 80 \times 105$ mm 3 , $100 \times 70 \times 105$ mm 3 , $100 \times 80 \times 60$ mm 3 respectively. An iron plate with a thickness of 30 mm encloses the whole wiggler and acts as a magnetic yoke. There is an opening in the yoke face for the vacuum pipe of 32×120 mm 2 .

The magnetic design has been calculated by a 3D code for 4 periods. The pole shape has been optimized to improve the width of the good- field region in the transverse direction, by means of 4 shims, placed symmetrically about the longitudinal wiggler axis as shown in Fig.3. The total thickness of the shims is 0.6 mm, and therefore the gap at the wiggler center is increased to 33.2 mm. The size of the vacuum chamber is not considered in the analysis, but the gap of the poles should be 33.2 mm (larger than in the calculation) for an elliptic chamber.

The center field is correspondingly reduced by $\approx 3\%$. Fig.4 shows the vertical field component along the wiggler longitudinal axis.

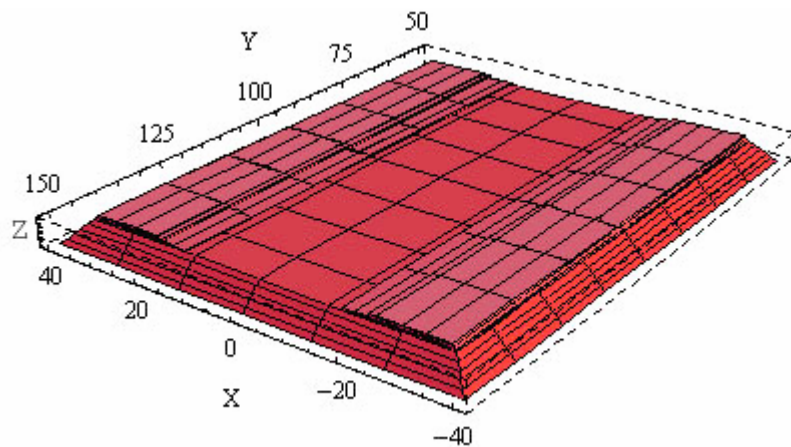


Fig. 3: Wiggler pole profile optimized with four shims.

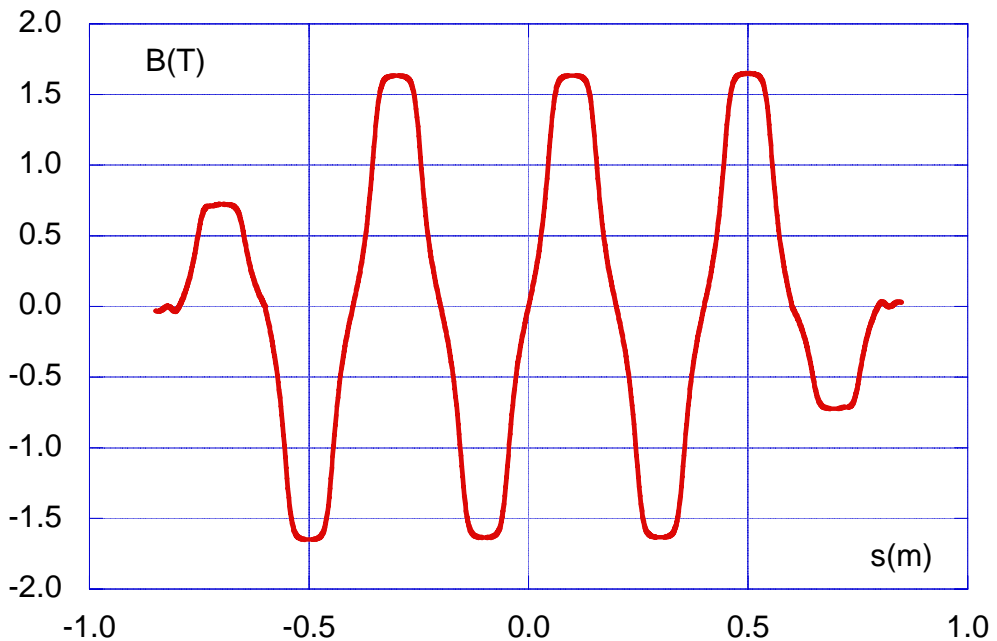


Fig. 4: Vertical field component on the wiggler axis

2 Field quality

The results of the optimization by means of the shims is summarized in Table 1; Fig.5 shows the behaviour of the vertical field component in the symmetry plane of the wiggler as a function of the horizontal position at the center of the pole up to ± 28 mm (twice the good field region) from the center and Fig.6 its relative deviation inside the good field region.

Table 1: Results of pole shimming.

	Without shims	With shims
Peak field at pole center (T)	1.684	1.635
$ \Delta B/B_0 $ @ 5 mm at pole center	4.3×10^{-4}	5.5×10^{-5}
$ \Delta B/B_0 $ @ 10 mm at pole center	2.3×10^{-3}	6.1×10^{-5}
$ \Delta B/B_0 $ @ 14 mm at pole center	5.6×10^{-3}	1.6×10^{-4}

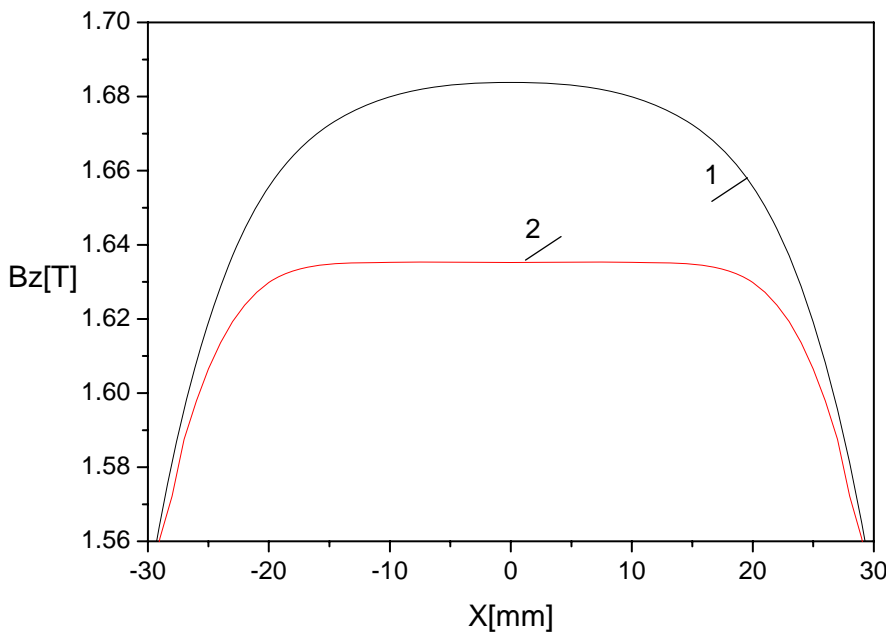


Figure 5: Vertical field component $B_z(x)$ in the orbit plane $Z=0$ at the pole center: 1—without shims, 2—with shims

Without shims of the vertical field component $B_z(x)$ at the pole center changes by 5.6×10^{-3} in the required good field region ($-14 \text{ mm} \leq X \leq 14 \text{ mm}$). With the shims $\Delta B/B_0$ is improved more than an order of magnitude and does not exceed 1.6×10^{-4} .

The conditioning of vanishing angle of the reference beam trajectory at the end of the wiggler comes naturally from the antisymmetric shape of the field with respect to the magnet center. The additional condition of vanishing displacement (second field integral) is obtained by trimming the shape of the end poles. This is made by eliminating the top magnet and reducing the height of the side ones (see Fig.1). The reference trajectory of the beam inside the wiggler

is shown in Fig.7, while Fig.8 gives the behaviour of the radiation integral $I_D = \int B_z^2 dz$, which exhibits a step-like shape with a growth value of $0.56 T^2 m$ per period, i.e. $1.4 T^2 m$ per meter.

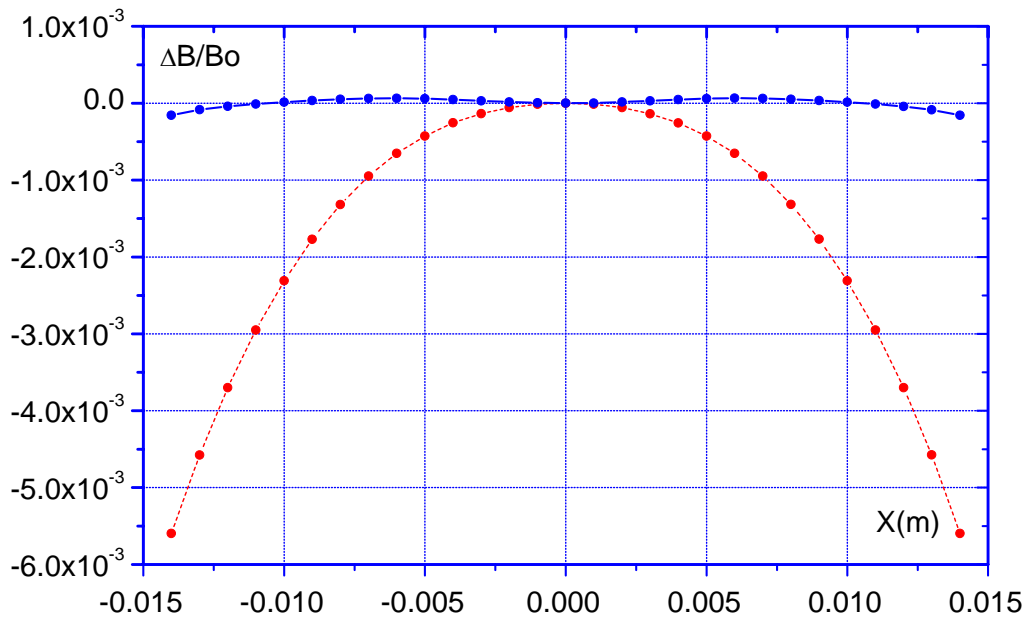


Fig.6: Relative change of magnetic field in transverse direction at the pole center:
Dotted line = without shims, full line = with shims.

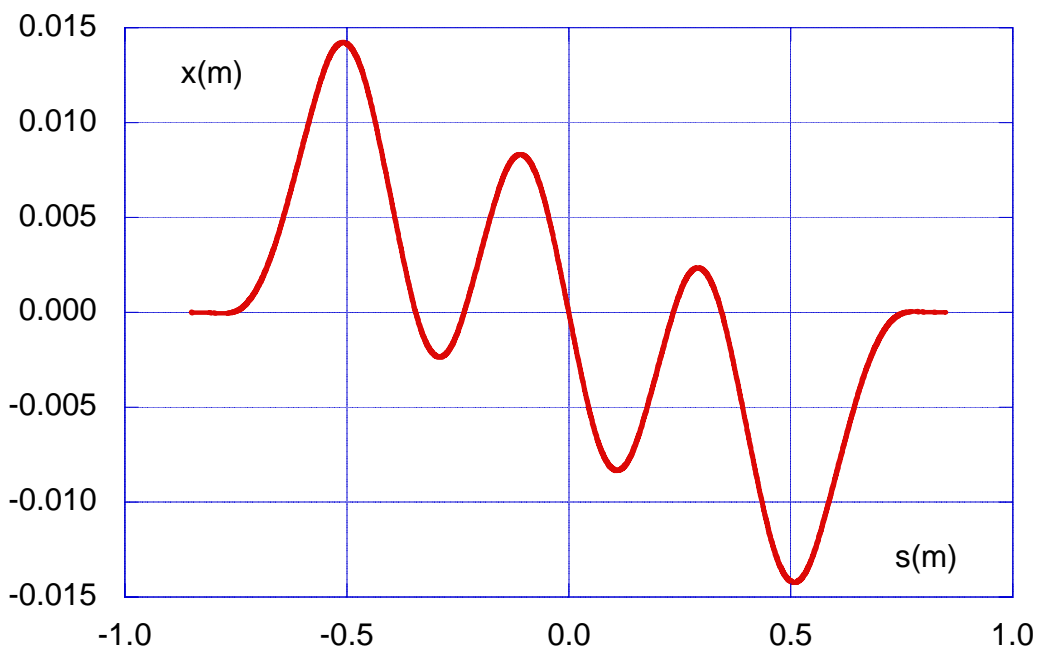
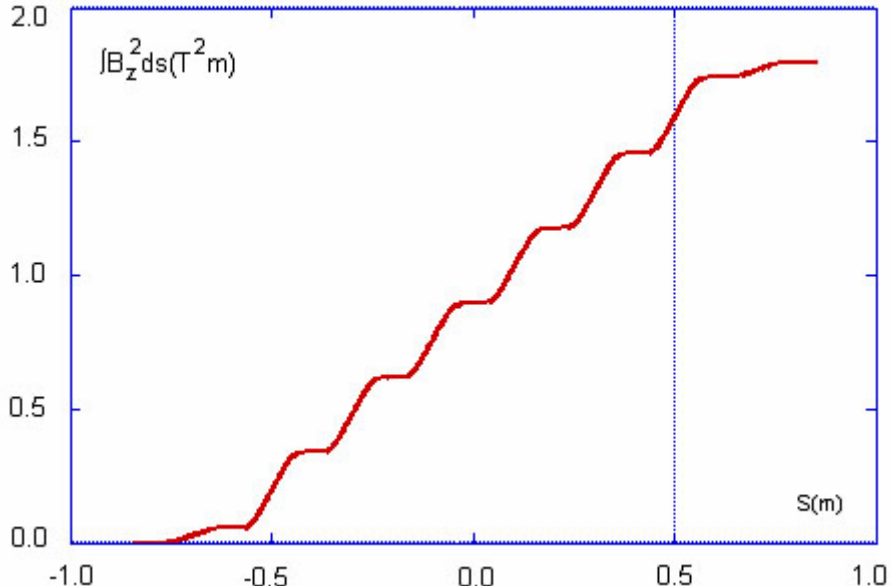


Fig.7: Reference beam trajectory inside the wiggler

Fig.8: Damping integral $I_D = \int B_z^2 ds$

In order to estimate the contribution of high order terms in the magnetic field of the wiggler, it is necessary to analyze the field in the whole magnet. We have therefore fitted the points at the same longitudinal positions but different horizontal ones in the wiggler midplane with a fourth order polynomial around the reference trajectory x_t of the beam inside the wiggler

$$B_z(x, s) = b_0(s) + b_1(s)(x - x_t) + b_2(s)(x - x_t)^2 + b_3(s)(x - x_t)^3 + b_4(s)(x - x_t)^4$$

repeating the procedure for all the longitudinal positions in the mesh calculated with the 3D code. The behaviour of $b_0(s)$ is practically identical to the field calculated on the wiggler axis (see Fig.4). Figs. 9,10,11,12 show the other coefficients, while Fig.12 represents the average deviation between the calculated points and the fit. Table 2 gives the values of the coefficients integrated along the beam trajectory in the wiggler. Only odd terms are present because of the antisymmetric behaviour of both field and beam trajectory. The same quantities calculated for the previous proposal [1] are shown in the third column.

Table 2 – Integrated polynomial coefficients

	Without shims	With shims	Previous proposal
$\int b_1 ds (Tm)$	0.040	0.026	0.029
$\int b_3 ds (T/m^2)$	120.08	27.11	255.60

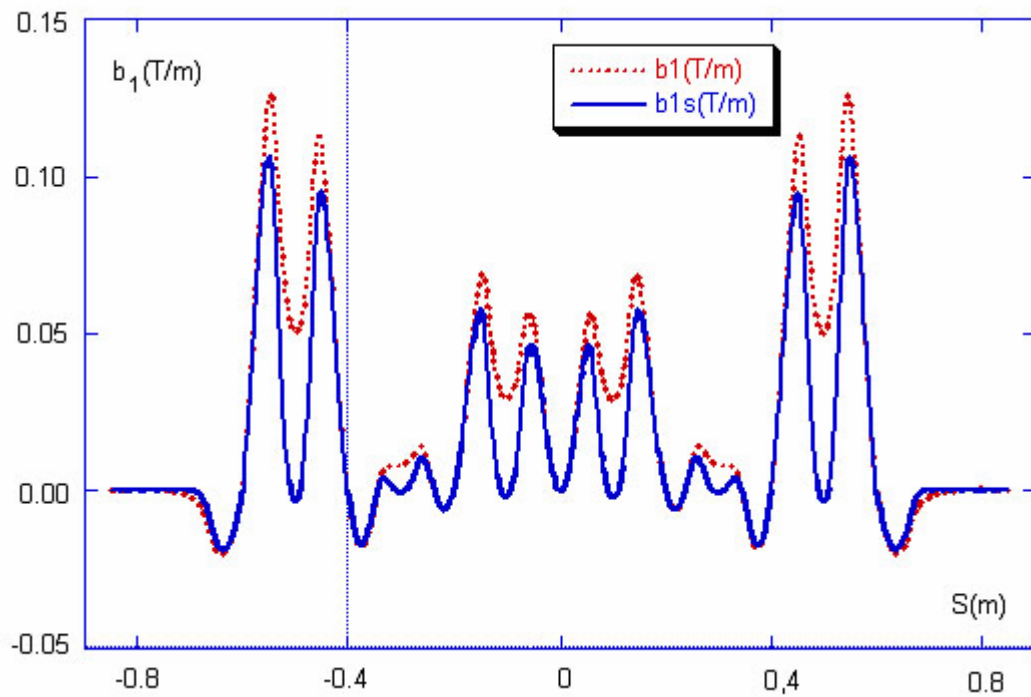


Fig.9: First order coefficient along the beam trajectory in the wiggler
 Dotted line = without shims; full line= with shims

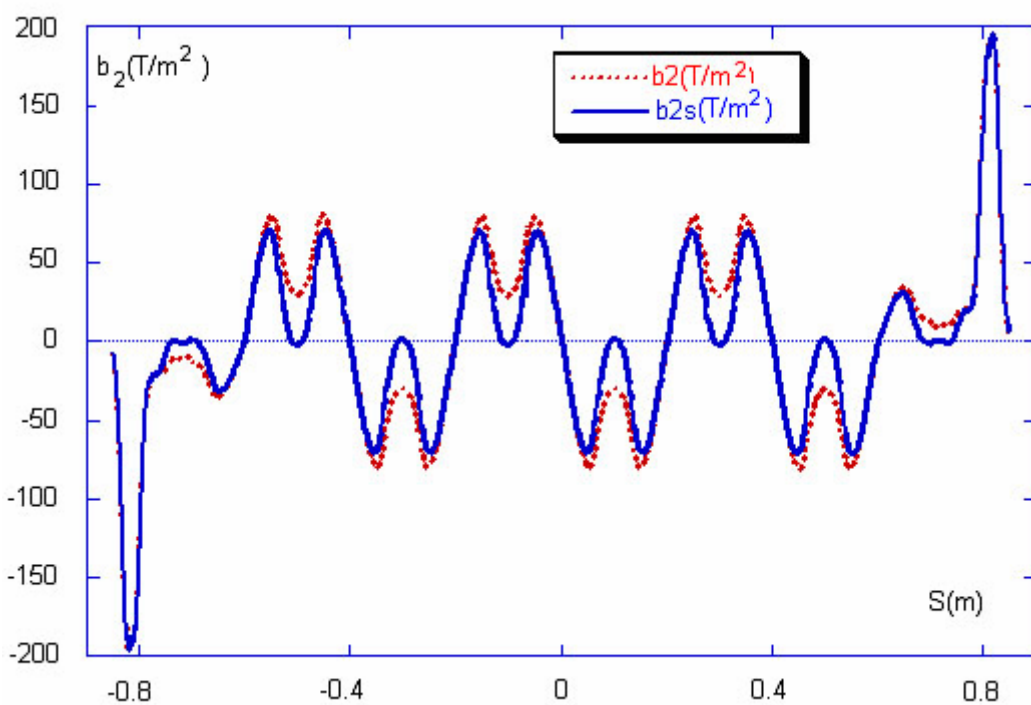


Fig.10: Second order coefficient along the beam trajectory in the wiggler
 Dotted line = without shims; full line= with shims

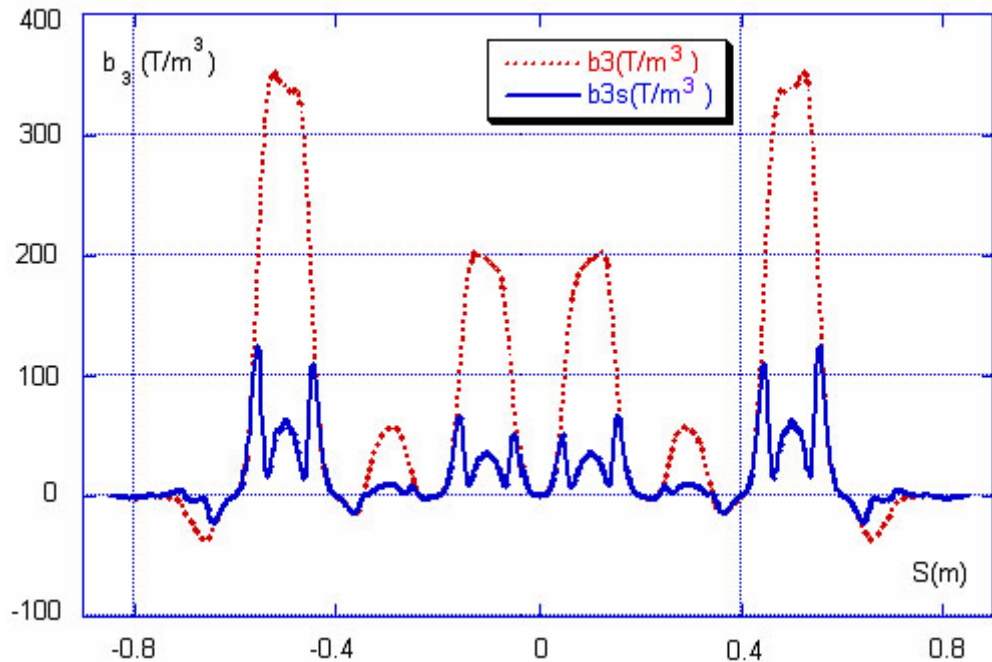


Fig.11: Third order coefficient along the beam trajectory in the wiggler
 Dotted line = without shims; full line= with shims

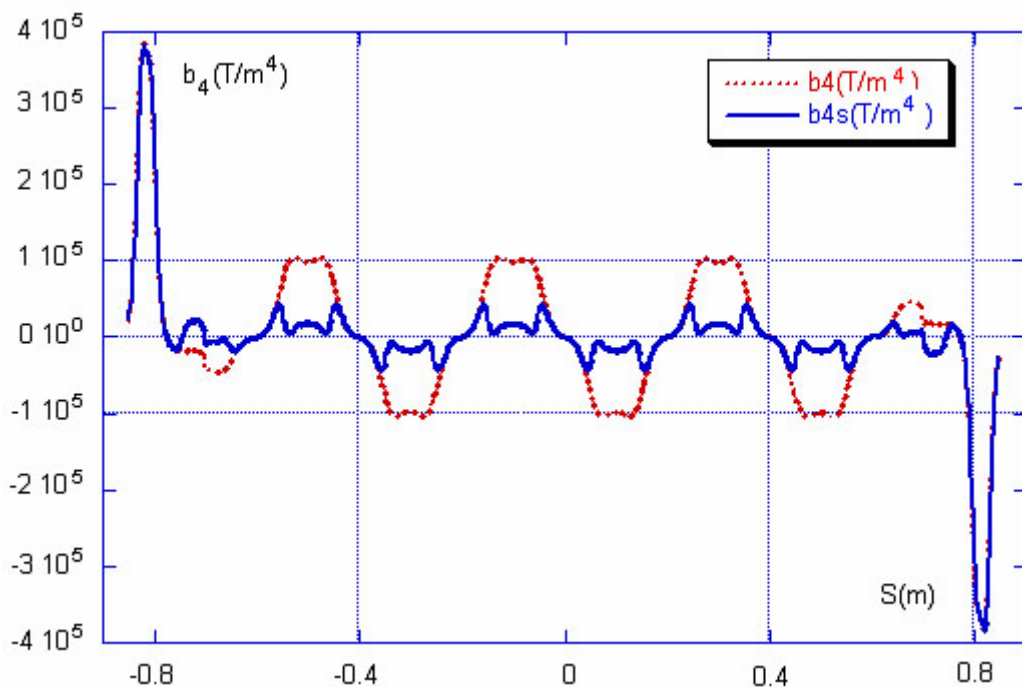


Fig.12: Fourth order coefficient along the beam trajectory in the wiggler
 Dotted line = without shims; full line= with shims

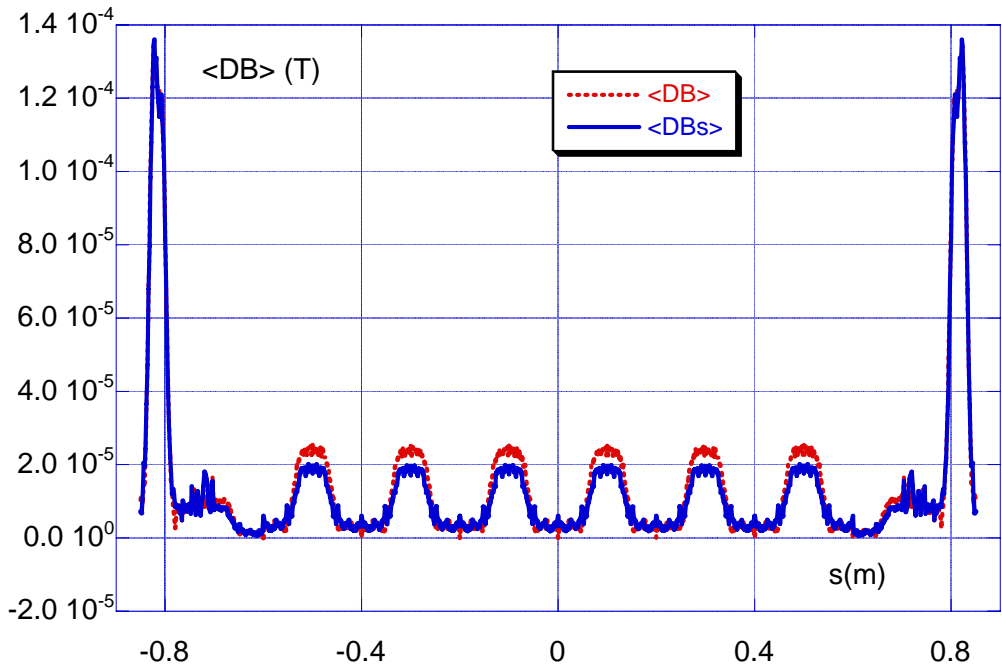


Fig.13: Average difference between calculated and fitted field values
 Dotted line = without shims; full line= with shims

3 Conclusion

A new hybrid magnet solution for the ILC damping rings wiggler has been designed to match the tight tolerances on the good field region imposed by the requirements on the dynamic aperture of the ring. Increased pole width and magnet gap, together with a careful design of correcting shims provide a much better field quality with respect to the previous proposal [1].

Acknowledgement

This work is supported by the Commission of the European Communities under the 6th Framework Programme “Structuring the European Research Area”, contract number RIDS-011899.

References

[1] A. Babayan, D. Melkumyan, V. Nikoghosyan “Wiggler Magnet Optimization for Linear Collider Damping Ring” EUROTeV-Report-2006-011